

Supplement of Biogeosciences, 16, 77–103, 2019
<https://doi.org/10.5194/bg-16-77-2019-supplement>
© Author(s) 2019. This work is distributed under
the Creative Commons Attribution 4.0 License.



Supplement of

Optimal inverse estimation of ecosystem parameters from observations of carbon and energy fluxes

Debsunder Dutta et al.

Correspondence to: Debsunder Dutta (debsunder.dutta@jpl.nasa.gov)
and Christian Frankenberg (cfranken@caltech.edu)

The copyright of individual parts of the supplement might differ from the CC BY 4.0 License.

S1 Comparison of Old and New Photosynthesis Implementations in SCOPE

To study the overall or net response from the SCOPE model in terms of canopy level fluxes, we tested the old and new model version for both C_3 and C_4 species at two different sites. Figure S1 shows the comparison of SCOPE model predictions for both model versions using C_4 plants. The results shown are for corn (C_4) crops at the Mead-1 Ameriflux site in Lincoln, Nebraska (see section 6.3.1 main text for some more site information). The environmental forcings and SCOPE parameterizations (un-optimized) were kept identical for the old and new SCOPE runs. The only difference is the replacement of the old biochemical module with our new photosynthesis implementation. The top panel shows the environmental forcing for a few clear days in the growing season. There is considerable variability in temperature and VPD. The middle and lower panels represent the comparisons in diurnal GPP and LE fluxes. It is observed that with the given parameterization the newer implementation better captures the diurnal variability as compared to the actual tower observations at relatively higher average canopy temperatures.

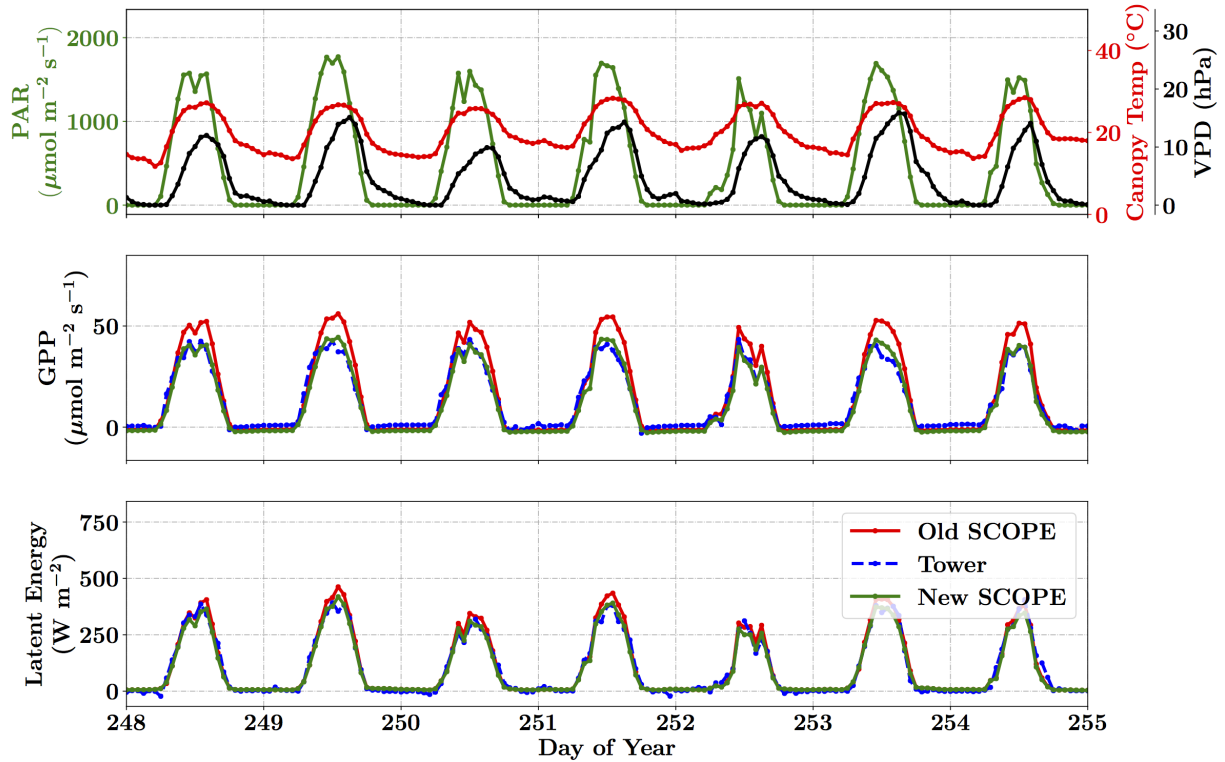


Figure S1. Figure showing the diurnal variability in SCOPE model simulations for C_4 corn species at the Nebraska, Mead-1 site for a week in the growing season for the year 2009. The top panel shows the variability of a few important meteorological forcing variables. The middle and lower panels show the variability in the diurnal cycle of GPP and latent energy respectively as a comparison between the old and new photosynthesis implementations (for identical parameterization and forcings) in SCOPE and the actual tower observed values.

10

Figure S2 shows similar plots and comparisons as described above in terms of f_{GPP} but for corn (C_4) crop grown at the Mead-1 Ameriflux site in Nebraska Lincoln (see section 6.3.1 main text for some more site information). It appears from the results that there is only a decrease in canopy GPP for the new SCOPE both in the space of PAR-Canopy Temperature and PAR-VPD by about 5-30%, which can be attributed to photosynthesis being limited by light instead of rubisco at higher temperatures. As mentioned previously, there is uncertainty associated with these contour diagrams although these are quite small (< 10%) and it is found that these patterns are also nearly the same (not shown).

15

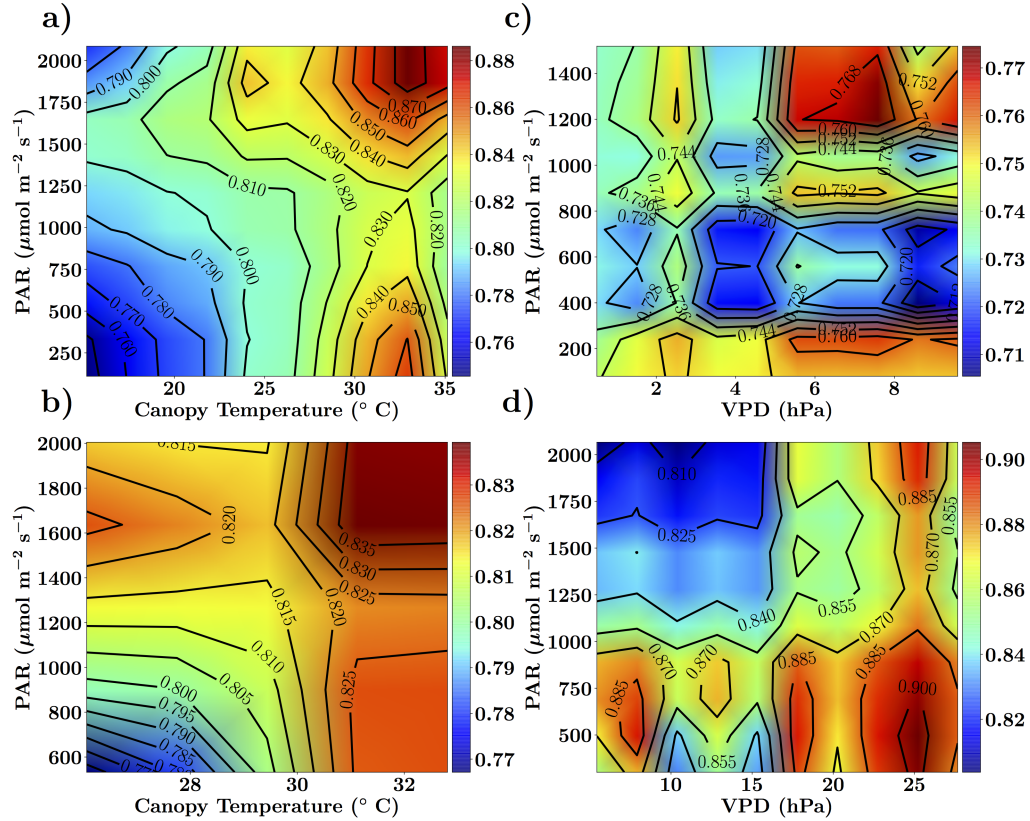


Figure S2. Figure showing the ratio of old and new SCOPE GPP ($f_{GPP} = \frac{GPP_{new}}{GPP_{old}}$) simulations as a function of PAR, canopy temperature and VPD for the C_4 species. The Nebraska Mead-1 site with corn growing for the year 2009 is used and the SCOPE simulations are driven with identical forcings and parameters for both the new and old simulations, the only difference being the implementation of photosynthesis and its temperature dependence (see text). The left column shows f_{GPP} as a function of PAR and canopy temperature with data points in the low VPD range of 10-15 hPa (panel-a) and high VPD range of 25-30 hPa (panel-b). The right column shows f_{GPP} as a function of PAR and VPD with data points in the low temperature range of 10-15 °C (panel-c) and high temperature range of 30-35 °C (panel-d).

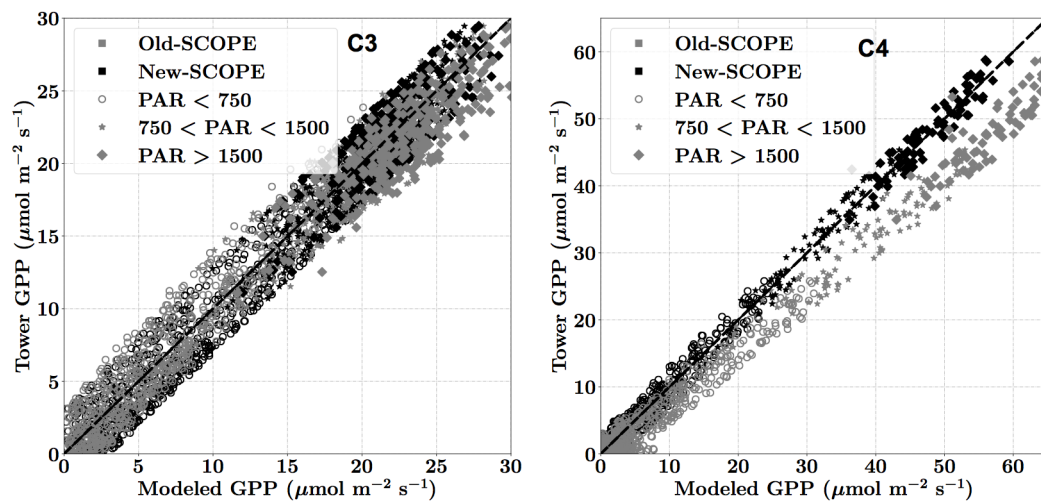


Figure S3. Figure showing the comparison of the tower observed vs modeled canopy GPP for new and old Photosynthesis implementations in the SCOPE model. The results are shown for both the C₃ (left) and C₄ (right) species. The model simulations for the C₃ species are for the Missouri Ozark Site comprising of Deciduous Broadleaf Forests, the C₄ simulations are for the Nebraska Mead-1 site with corn growing both for the year 2009.

Figure S3 shows the modeled vs observed comparison for new (as per CLM4.5) and old (previous) implementation of photosynthesis in SCOPE for both the C_3 and C_4 species. We select a set of points (time indices) from the new SCOPE simulations at various PAR ranges whose modeled GPP fluxes are very close to the tower observed values. The points corresponding to the same time indices from the old SCOPE simulations are then selected for comparing the modeled GPP. It is found that for C_3 species there is not much change but for C_4 species the new SCOPE GPP values are generally reduced. This result is also in agreement with the contour plots as presented in Fig. S2.

S1.1 Retrieval Results for the Missouri Ozark site

S1.1.1 Site Description

The top two panels (Figure S4, S5) show the environmental forcing variables which (except precipitation) are used as input in the SCOPE model simulations. The bottom panel represents the observations of carbon (GPP) and energy (LE, H) fluxes which are used to construct the observation vector Y (composed of GPP and LE data concatenated together) for each of the windowed inversions. The growing season is longer for this site from around March, when the air temperatures starts to become positive and slightly warmer, till around November when the trees lose leaves and there is onset of the fall season. Site temperatures are quite high with high VPD around June and July. Again, we focus on the retrieval of the parameters V_{cmax} , BB_{slope} and LAI during this entire longer growing season.

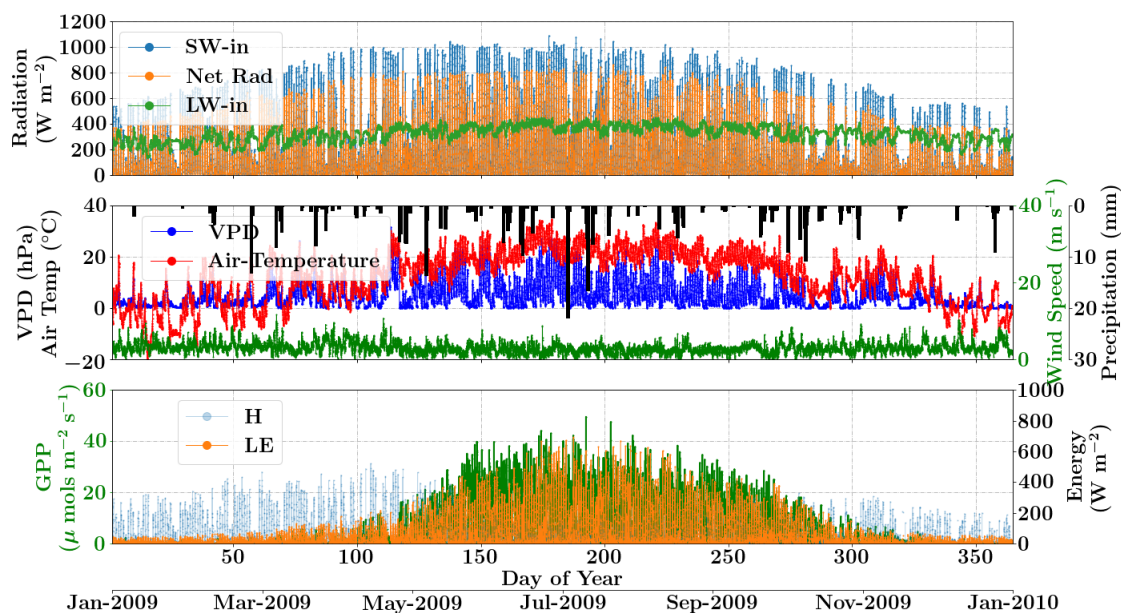


Figure S4. Figure showing the diurnal and seasonal variability of important environmental and meteorological forcings together with the tower observed fluxes of carbon and energy used in SCOPE model inversions for the Missouri Ozark flux tower site for the year 2009. The variables in the top and middle panels are used as inputs to the SCOPE model and the variables in bottom panel is used as a target in a moving window retrieval approach.

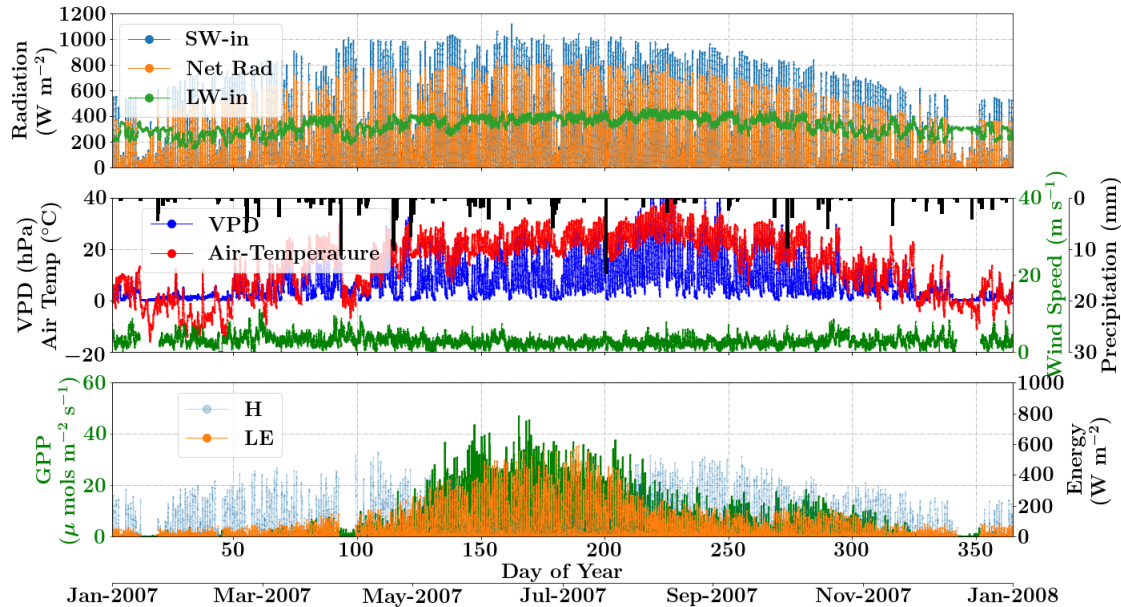


Figure S5. Figure showing the diurnal and seasonal variability of important environmental and meteorological forcings together with the tower observed fluxes of carbon and energy used in SCOPE model inversions for the Missouri Ozark flux tower site for the year 2007. The variables in the top and middle panels are used as inputs to the SCOPE model and the variables in bottom panel is used as a target in a moving window retrieval approach.

S1.1.2 Effect of Temperature Dependence on Parameter Retrievals

Sensitivity analysis of the newer temperature dependence of photosynthesis parameterization in SCOPE implemented in this study to inversion parameter retrievals is performed. We use the dataset from Ozark for the year 2010. The Inversion is performed with the 3-day window setup and conditions as presented in section 6.4. The retrievals are successively computed with and without the temperature dependent responses with other conditions identical and a posterior simulation is performed with the optimized parameters. Figure S9 shows the average canopy temperature from posterior simulations with the photosynthetic temperature dependence. As a comparison the surface temperature computed from outgoing longwave radiation from flux tower observations (assuming emissivity of 0.95) is also plotted. SCOPE seems to track the canopy temperatures well, the slightly higher temperatures at the mid-day can be attributed to the mixed effect of soil which is captured by the tower observations. The 3-day windowed retrievals of V_{cmax} with and without temperature dependence are shown with soil and broken dark green lines. The light green lines represent the half hourly expected V_{cmax} computed with the response functions B1 and B2 (presented in the appendix) and the canopy temperature profile (grey lines). The broken red line represents the 3-day average V_{cmax} . The method although does not reflect the actual non-linear transformations for V_{cmax} but the values tend to shift towards L1 with increased correlation which also follows the variability (L1) well. Figure S10 shows the one to one plots of the posterior model simulations with and without temperature dependent corrections (TDC) and its comparison with the flux tower observations for both GPP and LE fluxes. The results are found to be better when the temperature dependence corrections are implemented with improved R^2 values and the following error measures, $\chi_{GPP-TDC}^2 = 26631$, $\chi_{GPP-NTDC}^2 = 30046$, $\chi_{LE-TDC}^2 = 29766$ and $\chi_{LE-NTDC}^2 = 31870$.

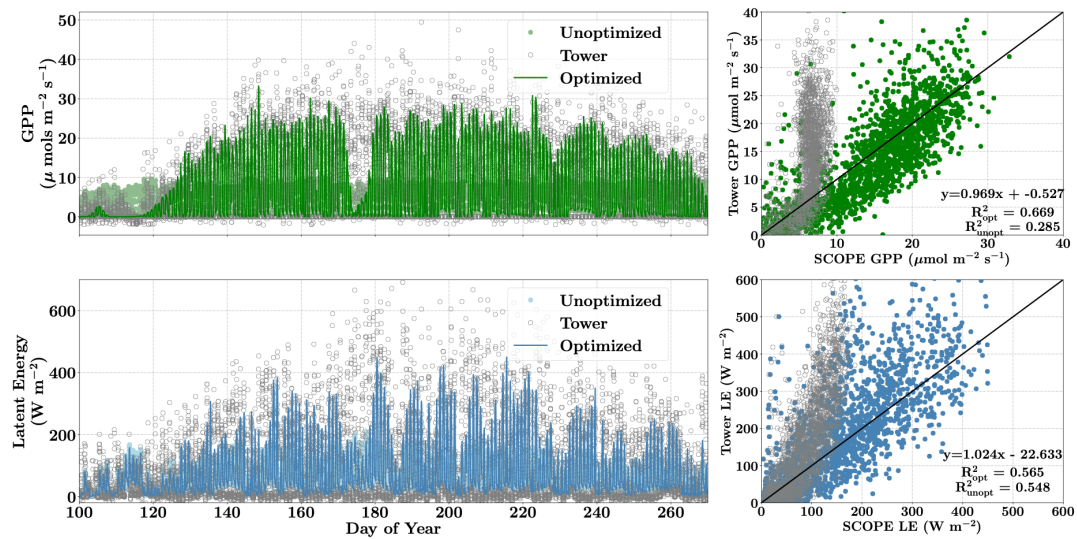


Figure S6. Figure showing the improvement in diurnal and seasonal variability in modeling the GPP and LE fluxes with optimized parameters over prior values using SCOPE for the Missouri Ozark site for the year 2009. The figure also shows the one-to-one comparison (indicated by black-line) with the observed flux tower values. The optimization of the photosynthetic parameters improves the accuracy of computing the carbon and water fluxes as indicated by the R^2 value and the equation of the regression line.

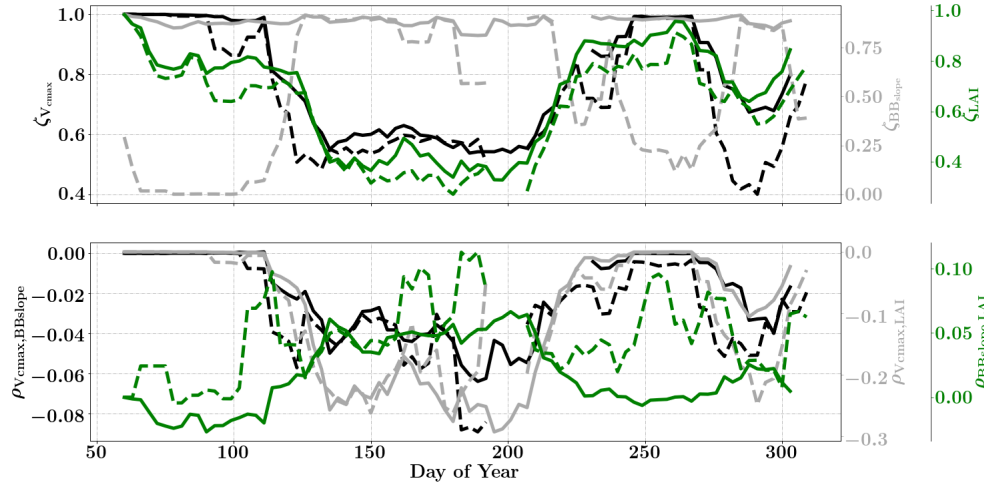


Figure S7. Figure showing the seasonal variability of the posterior error reduction (ζ) and correlation coefficient of the retrieved parameter values of V_{cmax} , BB_{slope} and LAI for the Missouri Ozark site using a 3-day moving window inversion approach for the year 2007. The top panel shows the $\zeta_{V_{cmax}}$, $\zeta_{BB_{slope}}$ and ζ_{LAI} for the entire growing season and the bottom panels shows the correlation coefficients (normalized off-diagonal elements of posterior error covariance matrix) among these variables. The results of retrievals using only GPP and LE fluxes are shown as dashed lines and the results using a combination of fluxes and MODIS reflectance are shown as solid lines. Both the ζ and correlation coefficients are computed using the final Jacobian matrix at the end of each retrieval window.

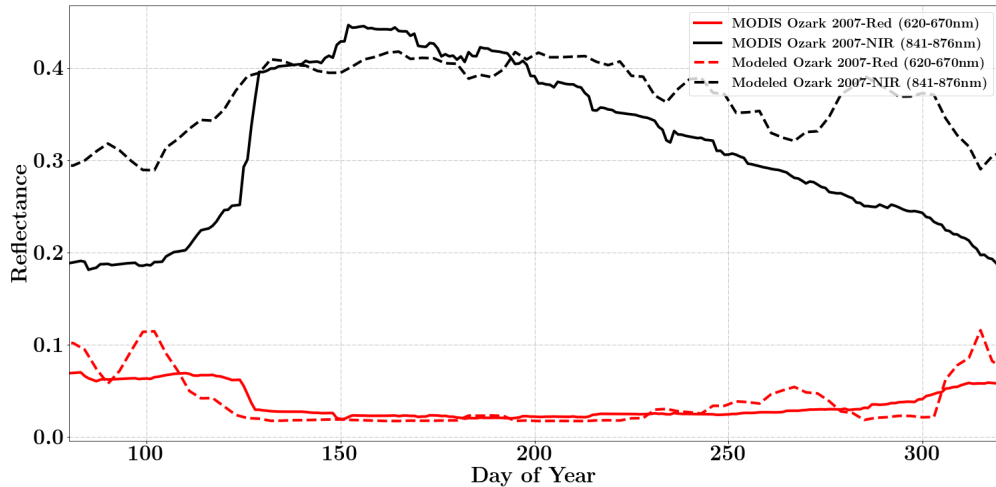


Figure S8. Figure showing the seasonal variability of modeled red and NIR channels of MODIS using optimized SCOPE parameters V_{cmax} , BB_{slope} and LAI. The values are also compared with actual observations from the satellite. It is found that the inversions match the red reflectance observations extremely well and NIR observations fairly well.

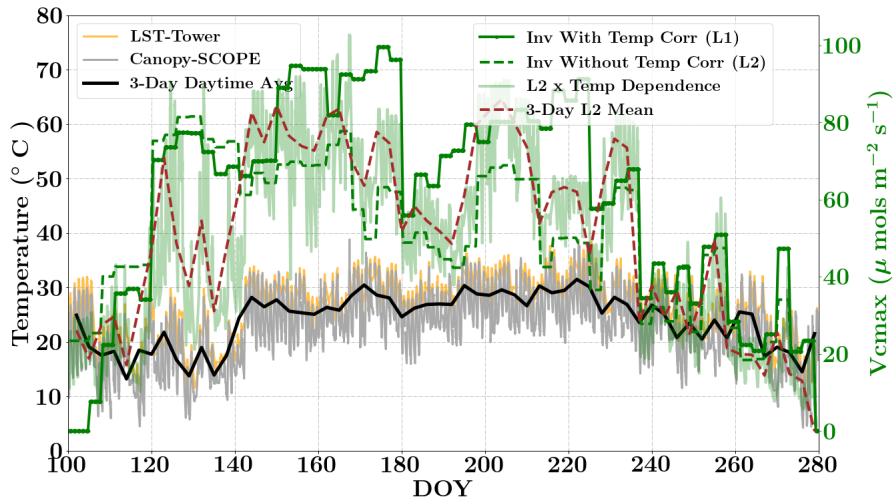


Figure S9. Figure showing the seasonal variability and comparison of the retrieved V_{cmax} with (L1) and without (L2) temperature dependence implementation in the SCOPE inversion framework. The results indicate that SCOPE is able to model the average canopy temperatures well as compared to flux tower observations. The differences in the retrieved V_{cmax} are pronounced during the middle of the growing season and further convolution of L2 with temperature dependence functions shifts the variability of V_{cmax} towards L1 (broken red line).

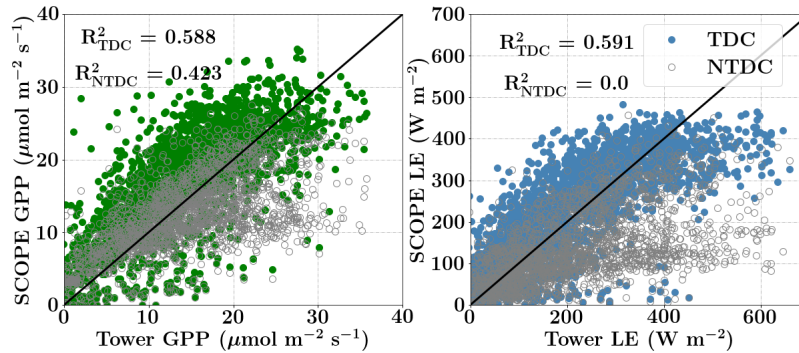


Figure S10. Figure showing the one-to one comparison of posterior simulation of GPP and LE fluxes with flux tower observations for the Missouri Ozark site for the year 2010. The parameter optimizations are performed with (TDC) and without (NTDC) temperature dependent corrections of photosynthetic parameters in the inversion framework. The results clearly show improvement with the temperature dependent corrections incorporated in the inversions.

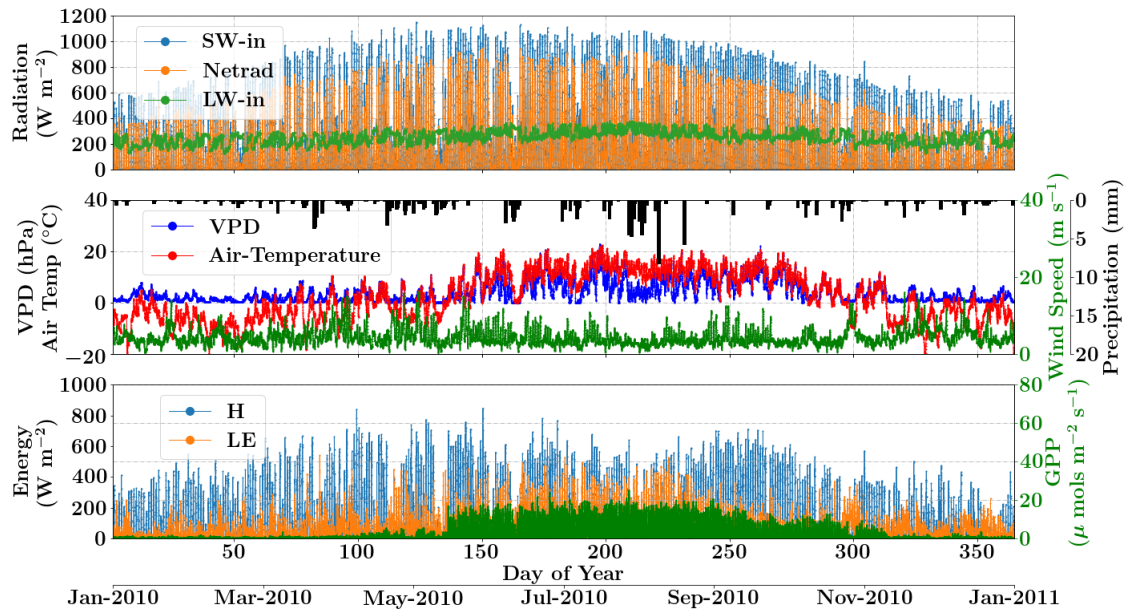


Figure S11. Figure showing the diurnal and seasonal variability of important environmental and meteorological forcings together with the tower observed fluxes of carbon and energy used in SCOPE model inversions for the Niwot Ridge flux tower site. The top two panels show the environmental forcing variables which (except precipitation) are used as input in the SCOPE model simulations. The bottom panel represents the observations of carbon (GPP) and energy (LE, H) fluxes which are used to construct the observation vector Y (composed of GPP and LE data concatenated together) for each of the windowed inversions.